

PARAMETER OPTIMIZATION IN THE REGULARIZED KERNEL MINIMUM NOISE FRACTION TRANSFORMATION

Allan A. Nielsen*

Technical University of Denmark
DTU Space – National Space Institute
Asmussens Allé, Building 321
DK-2800 Lyngby, Denmark

Jacob S. Vestergaard

Technical University of Denmark
DTU Informatics – Informatics and
Mathematical Modelling
Asmussens Allé, Building 321
DK-2800 Lyngby, Denmark

1. INTRODUCTION

Based on the original, linear minimum noise fraction (MNF) transformation [1] and kernel principal component analysis [2], a kernel version of the MNF transformation was recently introduced [3, 4]. Inspired by [5] we here give a simple method for finding optimal parameters in a regularized version of kernel MNF analysis. We consider the model signal-to-noise ratio (SNR) as a function of the kernel parameters and the regularization parameter. In 2-4 steps of increasingly refined grid searches we find the parameters that maximize the model SNR. An example based on data from the DLR 3K camera system [6, 7] is given.

2. THE KERNEL MNF TRANSFORMATION

In a regularized version of the kernel MNF transformation we maximize the Rayleigh quotient [3, 4]

$$\frac{1}{\text{NF}} = \frac{b^T K^2 b}{b^T [(1 - \lambda) K_N K_N^T + \lambda K] b}, \quad (1)$$

i.e., the inverse noise fraction, NF, here defined as the variance of the noise according to some noise model divided by the variance of the total. K and K_N are centered kernelized versions of the data and the noise part, respectively [3, 4]. This corresponds to maximizing the signal-to-noise ratio, $\text{SNR} = 1/\text{NF} - 1$. Alternatively, we may minimize the Rayleigh quotient

$$\text{NF} = \frac{b^T K_N K_N^T b}{b^T [(1 - \lambda) K^2 + \lambda K] b}. \quad (2)$$

Below we maximize the expression in Equation 1. We use a Gaussian kernel function $\kappa(x_i, x_j) = \exp(-\frac{1}{2} \|x_i - x_j\|^2 / \sigma^2)$, where x_i and x_j are vectors of observations, with $\sigma = s\sigma_0$ where σ_0 is the mean or the median distance between the observations in feature space and s is a scale factor.

3. SIMPLE PARAMETER OPTIMIZATION

We consider the model SNR as a function of the kernel parameter(s) and the regularization parameter, here $\text{SNR} = \text{SNR}(\sigma, \lambda) = \text{SNR}(s, \lambda)$. We use the mean for σ_0 and the residual from a fit

*Allan Aasbjerg Nielsen's e-mail address is aa@space.dtu.dk, his homepage is <http://www.imm.dtu.dk/~aa>.

to a quadratic in a 3 by 3 window as the noise. We start by calculating $\text{SNR}(s, \lambda)$ for discrete values of s and λ in crudely sampled intervals, here $s \in [0.1 \ 0.25 \ 0.5 \ 1.0 \ 2.0 \ 5.0 \ 10.0]$ and $\lambda \in [0 \ 10^{-9} \ 10^{-6} \ 10^{-3}]$. Based on the result we home in on the maximal SNR for either the leading factor or a combination (sums or products) of the first few factors by confining s and λ to more narrow and denser intervals and end up finding the values for s and λ that maximize SNR.

4. DATA AND PROCESSING

The images used were recorded with the airborne DLR 3K camera system [6, 7] from the German Aerospace Center, DLR. This system consists of three commercially available 16 megapixel cameras arranged on a mount and a navigation unit with which it is possible to record time series of images covering large areas at frequencies up to 3 Hz. The 1000 rows by 1000 columns example images acquired 0.7 seconds apart cover a busy motorway. Figure 1 shows the RGB images at two time points. The data were orthoprojected using GPS/IMU measurements and a DEM. For flat terrain like here one pixel accuracy is obtained. In these data, the change occurring between the two time points will be dominated by the movement of the cars on the motorway. Undesired, apparent change will occur due to the movement of the aircraft and the different viewing positions at the two time points. Figure 2 shows simple band-wise differences between data from the two time points.

Figure 3 shows (top) result of the initial crude optimization (λ along x-axis and s along y-axis), and (bottom) eigenvalues/SNRs for several choices of σ after final optimization (in all cases here we get $\lambda = 0$), see also Table 1. As in [3] calculations are based on ~ 1000 training samples.

Figure 4 shows leading kMNFs for the default ($s = 1$, top) and optimum for the products of the first nine kMNFs ($s = 1.5$, bottom) cases. In the upper-right 100×100 pixels no-change background the ratio between the variances of the leading kMNFs for the $s = 1.5$ and $s = 1$ cases is 13.72 corresponding to 11.37 dB constituting a considerably better noise suppression for the $s = 1.5$ case. (Compared to the linear model the noise suppression improvement measured in the same fashion for the $s = 1.5$ case is 37,623 or 45.75 dB.)

Description	s	σ	SNR [dB]	Colour in Figure 3
both first eigenvalue and sum of first nine eigenvalues	1.7	27.12	57.40	red
product of first nine eigenvalues	1.5	23.93	51.52	limegreen
mean (default)	1.0	15.95	40.66	black
median		10.49	38.28	orange
linear			18.60	blue

Table 1: SNR for leading factor ($\lambda = 0$ in all cases).



Fig. 1. DLR 3K camera system RGB images taken 0.7 seconds apart, note the moving cars on the motorway, 1000×1000 pixels.

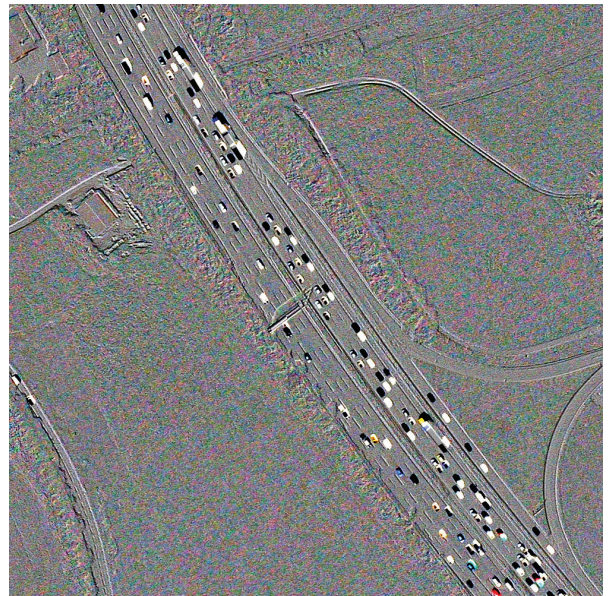


Fig. 2. Simple band-wise differences, note the noise in the no-change background.

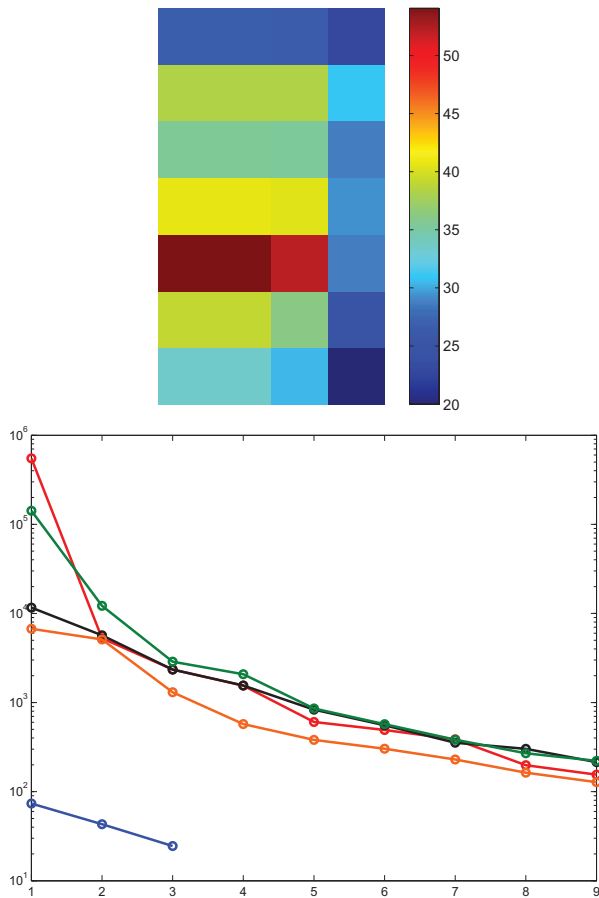


Fig. 3. Top: Initial crude optimization of model SNR over intervals $s \in [0.1 \ 0.25 \ 0.5 \ 1.0 \ 2.0 \ 5.0 \ 10.0]$ along the downward y-axis (the origo is in the top-left corner) and $\lambda \in [0 \ 10^{-9} \ 10^{-6} \ 10^{-3}]$ along the x-axis. Bottom: First few eigenvalues for several cases - optimum for both first eigenvalue and sum of first nine eigenvalues: $s = 1.7$, $\sigma = 27.12$, $\lambda = 0$ (red), optimum for product of first nine eigenvalues: $s = 1.5$, $\sigma = 23.93$, $\lambda = 0$ (limegreen), mean (default): $s = 1$, $\sigma = \sigma_0 = 15.95$, $\lambda = 0$ (black), median: $\sigma = 10.49$, $\lambda = 0$ (orange), linear MNF: $\lambda = 0$ (blue).

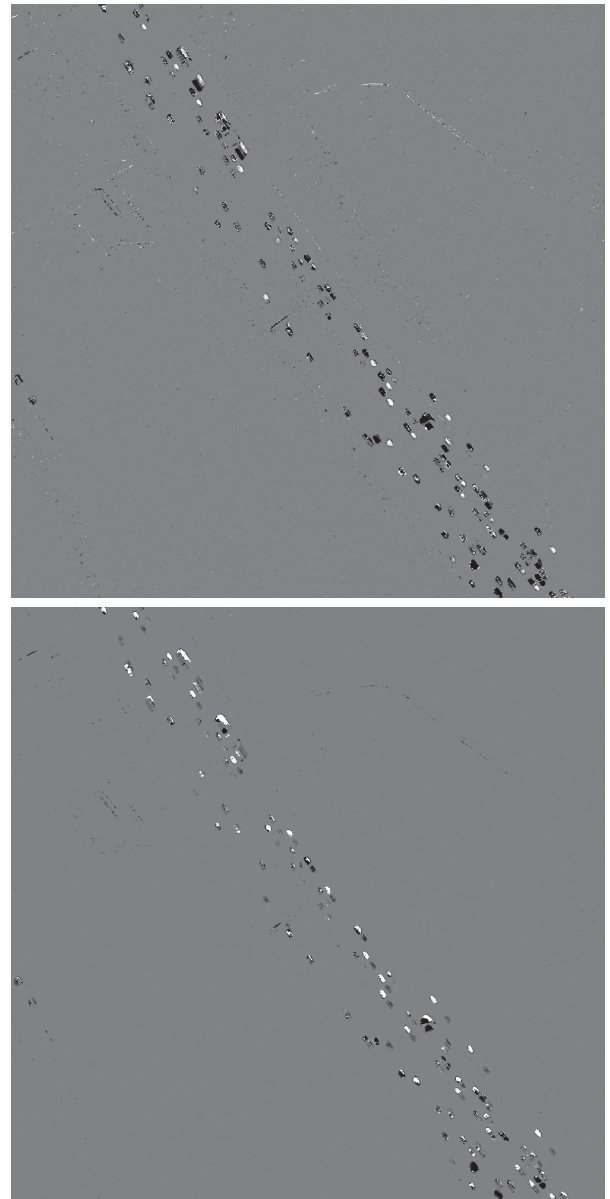


Fig. 4. Leading kMNFs for the default ($s = 1$, top) and the optimum for the products of the first nine eigenvalues ($s = 1.5$, bottom) cases ($\lambda = 0$ in both cases).

5. CONCLUSIONS

A simple method for optimization of kernel function and regularization parameters in the kernel MNF transformation is devised and applied to change detection in simple differences of bi-temporal DLR 3K camera system data. Figure 3 shows that although we get a much higher SNR for $s = 1.7$ than for $s = 1.5$ (57.40 dB vs 51.52 dB), the latter case because of the product applied, provides several (here four) eigenvalues higher than the default ($s = 1$) case. By coincidence, the two cases where we optimize SNR for the first factor only and where we optimize for the sum of the first nine factors, both give $s = 1.7$. In all cases here $\lambda = 0$.

Figures 3 and 4 show that with the suggested method, we obtain a clearly smoother background of no-change with a considerably better noise suppression at the potential risk of a few misses.

6. ACKNOWLEDGMENT

Dr. Peter Reinartz and coworkers, DLR German Aerospace Center, Oberpfaffenhofen, Germany, have kindly let us use the geometrically coregistered DLR 3K camera system data.

7. REFERENCES

- [1] A. A. Green, M. Berman, P. Switzer, and M. D. Craig, "A transformation for ordering multispectral data in terms of image quality with implications for noise removal," *IEEE Transactions on Geoscience and Remote Sensing*, vol. 26, no. 1, pp. 65–74, 1988.
- [2] B. Schölkopf, A. Smola, and K.-R. Müller, "Nonlinear component analysis as a kernel eigenvalue problem," *Neural Computation*, vol. 10, no. 5, pp. 1299–1319, 1998.
- [3] A. A. Nielsen, "Kernel maximum autocorrelation factor and minimum noise fraction transformations," *IEEE Transactions on Image Processing*, vol. 20, no. 3, pp. 612–624, 2011. <http://www.imm.dtu.dk/pubdb/p.php?5925>.
- [4] L. Gómez-Chova, A. A. Nielsen, and G. Camps-Valls, "Explicit signal to noise ratio in reproducing kernel Hilbert spaces," IEEE IGARSS, Vancouver, Canada, 25–29 July 2011. Invited contribution. <http://www.imm.dtu.dk/pubdb/p.php?6004>.
- [5] J. Trinder and M. Gomah, "Optimization and validation of support vector machines for land cover classification from aerial images and LiDAR data," 34th International Symposium on Remote Sensing of Environment (ISRSE), Sydney, Australia, 2011.
- [6] F. Kurz, B. Charmette, S. Suri, D. Rosenbaum, M. Spangler, A. Leonhardt, M. Bachleitner, R. Stätter, and P. Reinartz, "Automatic traffic monitoring with an airborne wide-angle digital camera system for estimation of travel times," in Photogrammetric Image Analysis, International Archives of the Photogrammetry, Remote Sensing and Spatial Information Service (PIA07), pp. 83–88, Munich, Germany, 2007.
- [7] F. Kurz, R. Müller, M. Stephani, P. Reinartz, and M. Schroeder, "Calibration of a wide-angle digital camera system for near real time scenarios," in ISPRS Workshop, High Resolution Earth Imaging for Geospatial Information, Hannover, Germany, 2007.